Experimental Astronomy manuscript No.
(will be inserted by the editor)

A XMM-Newton proton response matrix

Teresa Mineo · Simone Lotti · Silvano Molendi · Simona Guizzardi

Received: date / Accepted: date (Version 1.0 - 12 December 2016)

Abstract Soft protons constitute an important source of background in focusing X-ray telescopes, as Chandra and XMM-Newton experience has shown. The optics in fact transmit them to the focal plane with efficiency similar to the X-ray photon one. This effect is a good opportunity to study the environment of the Earth magnetosphere crossed by the X-ray satellite orbits, provided that we can link the spectra detected by the instruments with the ones impacting on the optics. For X-ray photons this link has the form of the so-called response matrix that includes the optics effective area and the energy redistribution in the detectors.

Here we present a first attempt to produce a proton response matrix exploiting ray-tracing and GEANT4 simulations with the final aim to be able to analyse XMM-Newton soft protons data and link them to the external environment. If the procedure is found to be reliable, it can be applied to any future X-ray missions to predict the soft particles spectra impacting on the focal plane instruments.

Keywords Background radiation · X-ray telescopes and instruments · X-ray

PACS 98.70.Vc · 95.55.Ka · 98.85.Nv

T. Mineo
INAF-IASF Palermo, via U. La Malfa 153, I-90146 Palermo, Italy Tel.: +39 091 6809478
Fax: +39 091 6882258
E-mail: mineo@iasf-palermo.inaf.it

S. Lotti,
INAF-IAPS, via del Fosso del Cavaliere 100, I-00113 Roma, Italy

S. Molendi, S. Guizzardi
INAF-IASF Milano, Via E. Bassini 15, I-20133 Milano, Italy

1 Introduction

The X-ray telescope capability of focusing protons with energies lower that a few hundreds keV was discovered just after *Chandra* X-ray observatory (Weisskopf et al. 2002) launch, when a rapid degradation of the front illuminated CCDs at the focal plane of the Wolter 1 telescope occurred (Lo and Srour 2003). The damages were caused by protons populating the radiation belts of the Earth magnetosphere crossed by the telescope during the perigee passage. XMM-Newton (Jansen et al. 2001) is exposed to the same risks being operated in a similar orbit but, in this case, instruments has been protected since the mission's start closing the filter wheel during the perigee passage and switching-off the detectors in case of intense solar activity. Soft proton contamination is observed also out of the radiation belts in form of flaring events during which the background rate can reach up to thousand times the quiescent level. These flares affect about 30-40% of the observing time and can last from hundreds of seconds to hours.

However, even if this effect degrades the telescope performances in observing X-ray sources, it could be a good opportunity to study the environment of the Earth magnetosphere crossed by the satellite orbits. The key in using the X-ray telescope as proton telescope is the capability in linking the spectra detected by the instruments with the ones impacting on the optics. This is possible by correctly modelling the physical processes involved in the interactions with all elements of the telescope.

The standard X-ray data analysis uses XSPEC (Dorman and Arnaud 2001) to obtain the spectrum emitted by the observed source from the detected one. Using this tool requires a response matrix that includes the specific characteristics of the instrument. In this paper, we present the simulations used to build a first version of a MOS response matrix to protons and a simple test on its validity, together with a discussion on some critical points still present in the procedure.

2 Physics interactions

XMM-Newton carries three X-ray telescopes each composed by 58 Wolter I grazing-incidence mirrors nested in a coaxial and cofocal configuration. The mirror shells have very shallow grazing angles ($\sim 30'$) in order to reflect photons up to 10 keV. Each telescope includes a baffle for visible and X-ray stray-light suppression. The detector at the focal plane, the European Photon Imaging Camera (EPIC), consists on three CCD cameras: two MOS (Metal Oxide Semi-conductor) CCDs and one pn CCDs array.

The MOS is an array of front illuminated CCDs with a sensitive silicon depth of 40 μm. The electrode has a complex structure. It is has a thinner layer that covers about 40% of the area with a 0.1 μm silicon and 0.15 μm silicon dioxide (open electrode); the normal electrodes that covers the other 60% of the surface has a thickness of 0.3 μm silicon and 0.75 μm silicon dioxide. The

MOS telescopes are equipped with a Reflection Grating Spectrometers (RGS) that intercepts about half of the X-ray light deflecting it to an off-set detector; photons imaging the MOS area (28.4′ diameter) are then 50% of the collected ones.

EPIC detectors are protected from the background induced by IR, visible and UV light with three optical blocking filters: the thin filter is made of 1600 Å polyimide film with 400 Å of aluminium evaporated on one side; the medium filter has 800 Å of aluminium deposited on the same material as the thin filter; and 1100 Å of aluminium and 450 Å of tin are evaporated on a 3300 Å polypropylene film for the thick filter.

The interaction of the protons with each single elements of the telescope is driven by different phenomena mainly because of the incident angles involved: the optics reflect protons coming at grazing incident angles, while the filter and the CCDs receive protons with almost normal directions.

The model for the proton interaction with the coated surface of the optics adopted in the production of the response matrix was derived by Remizovich et al. (1980) solving the transport equation for a proton beam in the elastic approximation. This model, valid for protons incident at small angles and with negligible loss of energy, assumes a total reflection probability of 100%: all incident particles are scattered. A beam with an incident polar angle ϑ_{in} and zero azimuthal angle has a scattering probability given by the following formula expressed in term of of the polar and azimuthal dimensionless variables ψ and ξ:

$$W(\psi,\xi) = \frac{1}{12\,\pi\,\psi^{1/2}}\left[\frac{\omega^4}{1+\omega^2} + \omega^3\,\arctan\omega\right] \tag{1}$$

with

$$\omega = \left\{\frac{3\,\psi}{\psi^2-\psi+1+(\xi/2)^2}\right\}^{1/2} \tag{2}$$

where ψ is the output polar angle normalized to the incident angle ($\psi = \vartheta_{out}/\vartheta_{in}$) and ξ the output azimuthal angle normalized to the polar incident angle ($\xi = \phi_{out}/\vartheta_{in}$). The scattering probability $W(\psi,\xi)$ is defined as the ratio of the rate of particles reflected in a given direction from a unit area to the rate of particles incident on the same area. Integrating Eq. 1 over ξ, the formula published by Firsov (1967) is obtained:

$$W(\psi) = \frac{3}{2\,\pi}\frac{\psi^{3/2}}{1+\psi^3} \tag{3}$$

Plots relative to the two functions are shown in the two panels of Fig. 2: the maximum scattering probability is obtained at output angles equal to the input ones.

The interactions with the filters and the CCD are treated through the stopping power, that is the energy loss due to Coulomb excitation and ionizations of the electrons in the medium, derived within the Bethe's theory (Bethe 1930). The processes are treated with Montecarlo methods using GEANT4

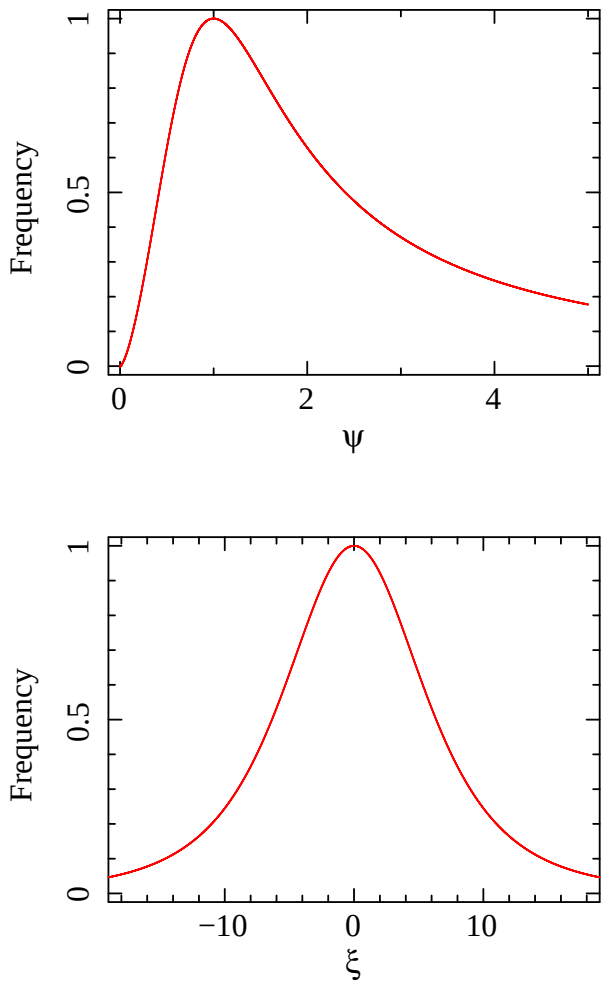

Fig. 1 Distribution probability for the proton scattering angles after the interaction with the optics. *Top panel:* Polar distribution integrated over the azimuthal angles as function of the dimensionless variable ψ. *Bottom panel:* Azimuthal distribution for ψ=1 as function of the dimensionless variable ξ.

(Allison et al. 2016, 2006; Agostinelli et al. 2003) for a precise calculation of the stopping power that depends on the particle energy.

3 The Simulators

The optics transmission was obtained with a ray-tracing Monte Carlo stand-alone code able to simulate either photons or protons. The code has already been used for the on-ground and in-flight calibration of the *Beppo*SAX (Conti et al. 1994) and Swift X-ray telescopes (Cusumano et al. 2006). It follows

the particle from the interaction with the mirror shells up to the focal plane taking into account the geometry of the optics, the effects of the baffle and the absorption from the uncoated back surface of the shells.

Protons with incident angles within the field of view of the telescope reach the focal plane after the interaction with the two mirror sections (double reflection). However, the focal plane can also be reached from angles out of the field of view after a single interaction with only one of the section of the mirror shells. The effect of these events is strongly limited by the presence of the baffle, but their contribution cannot be neglected. The parameter that better describe the optics transmission is the grasp $G(\vartheta, E)$ defined as:

$$G(\vartheta, E) = 2\,\pi \int_0^{\vartheta_{max}} A(\vartheta, E)\, \sin\vartheta\, d\vartheta \tag{4}$$

where E is the energy, $A(\vartheta, E)$ the effective area at the incident angle ϑ and $[2\,\pi\, \sin\vartheta\, d\vartheta]$ is the differential solid angle integrated up to the maximum off-axis angle ϑ_{max}.

We assumed a collecting radius at the focal plane of 3.25 cm, correspondent to $15'$, and simulated protons up to $\vartheta = 10°$. The grasp has a maximum value of 0.015 cm^2 sr as shown in Fig. 2 where it is plotted as function of the off-axis angles. It is independent on the proton energy because the adopted reflection model is obtained in elastic approximation.
A further reduction of 50% was included in the effective area to take into account the obscuration due to the gratings.

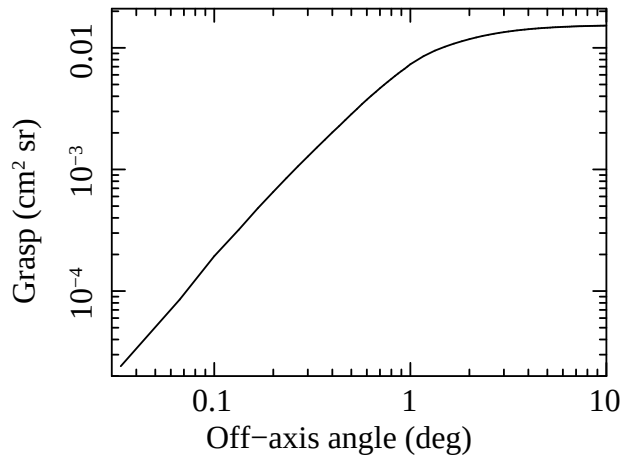

Fig. 2 XMM-Newton optics grasp as function of the off-axis angles computed with the ray-tracing.

The medium filter plus the electrode transmission was computed with Monte Carlo methods using a GEANT4 code. Protons crossing the filter lose on average 30 keV of their energy; in addition the open electrode absorbs on

average 30 keV while the normal electrode 120 keV. In addition, the transmission efficiency accounts for the fraction of events that deposit an energy in the range 0.2-10 keV. The plot in Fig. 3 gives the total transmission probability as function of the input proton energy. The two peaks are due to the structure of the MOS electrode. The peak with a maximum at ∼50 keV is due to protons that interact in the thinner section of the open electrode, while the higher energy peak is produced by protons impacting on the normal electrode.

The GEANT4 code is also used to obtain, for each input energy, the spectrum of the energies deposited in the MOS after crossing the filter and the electrodes necessary for building the redistribution matrix (see Sect. 4).

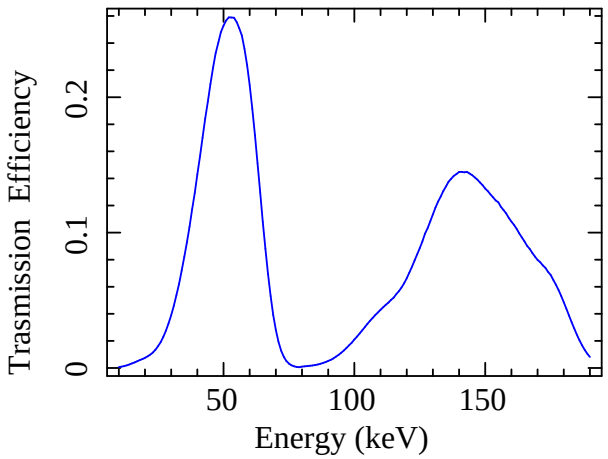

Fig. 3 Total transmission probability relative to the medium filter as function of the input proton energy. It accounts for the filter, the MOS electrode together with the factor for the fraction of events that are detected in the energy range 0.2-10 keV.

4 The MOS proton response matrix

The response matrix for the standard X-ray analysis contains the probability that an incoming photon of energy E is detected in the output detector channel PHA. To be used within XSPEC, the response matrix must be opportunely written in units of cm^2 according to the format required by the OGIP Calibration Memo CAL/GEN/92-002[1]. The MOS proton response matrix, was coded using the same definitions and format as for photons. The matrix is composed by two fits files:

– the ancillary response file (arf) that is an array that stores the summed contributions of all efficiencies. In the proton case, the arf file includes

[1] http://heasarc.gsfc.nasa.gov/docs/heasarc/caldb/docs/memos/cal_gen_92_002/cal_gen_92_002.html

as multiplicative factors the telescope grasp, the grating obscuration factor, the medium filter and the electrodes transmission efficiency and the probability that an absorbed proton is detected in the MOS working range 0.2-10 keV.

– the detector redistribution matrix file (rmf) that stores in a 2-d array (energy vs PHA channel) the probability that a proton with energy E_o is detected in the channel PHA correspondent to the energy E_d. The matrix has 180 rows each correspondent to a proton energy in the range 10-190 keV and 256 PHA output channels uniformly distributed in the range 0.2-10 keV. All rows are normalized to one.

The redistribution matrix relative to the input proton energy of 30 keV is shown in Fig. 4: the deposited energy with the highest probability corresponds to the PHA channels of ∼1 keV.

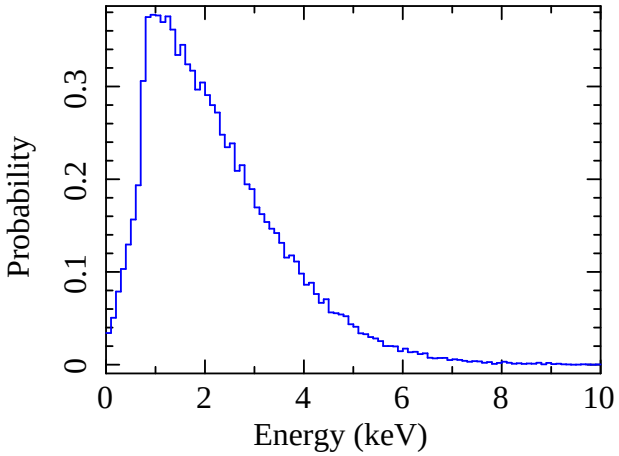

Fig. 4 Row of the redistribution matrix correspondent to the proton incident energy of 30 keV.

5 Comparison with real data

The quiescent soft proton spectrum published by Leccardi and Molendi (2008) is considered to validate and test the matrix. It is relative to MOS blank field observations for a total exposure of ∼600 ks and it was accumulated in the outer 10′-12′ ring of the detector. Counts in the spectrum can be modelled with a broken power law with a break energy at 5.0 keV, and the slopes fixed to 0.4 below 5 keV and 0.8 above 5 keV; the normalization at 1 keV of the MOS1 spectrum with the medium filter is $2.6\times10^{-3}\pm0.1\times10^{-3}$ count s^{-1} keV^{-1} (Leccardi and Molendi 2008).

In order to compare this spectrum with the one obtained with our simulation, a factor due to the different selection regions must be taken into account

in addition to the transmission efficiency obtained with the simulators. In a first approximation, this factor (0.19) is simply given by the ration between the annulus used to accumulate the spectrum (inner radius $10'$; outer radius $12'$) and the region assumed in the production of the matrix (a circle with $15'$ radius).

Using the proton response matrix within XSPEC and assuming a simple power law as input spectrum, a flux of 420^{+234}_{-153} pr cm^{-2} s^{-1} keV^{-1} sr^{-1} and a spectral index of 1.5±0.1 were obtained, where the errors are relative to 90% confidence level. Similar values of spectral index have been measured by several authors (Mewaldt et al. 2007; Dayeh et al. 2009) during quiet intervals.

6 Critical points

This first version of a proton response matrix, even if encouraging, has several critical points that should be addressed and solved in the future versions:

- the model adopted for the reflection must be validated by experimental measurements. A comparison was performed with measurements performed on one of the eROSITA shells with protons at energies of 250 keV, 500 keV and 1 MeV and off-axis angles between 0.3° and 1.3° (Diebold et al. 2015). The reflection model adopted in the ray-tracing reproduces the experimental results at angles ≃1° while overestimates the efficiency at lower angles. In addition an energy loss up to maximum of 20% is observed at all energy and angles. More dedicated measurements should be compared with the theoretical models in order to choose the one that better describes the interactions
- being the optical blocking filter and the electrodes quite thin, the straggling effects play an important role and GEANT4 precision in modelling the transmission could not be adequate. Dedicated measurements, again, would validate the function.
- several proton spectra, relative to magnetosphere regions and observing periods where the input spectrum to XMM-Newton satellite is known with acceptable precision, should be used to validate the matrix.

7 Conclusion

Results obtained with this first version of the soft proton response matrix provide an indication that it could be a powerful tool to derive the proton spectra in the magnetosphere regions crossed by the satellite, provided that all critical points presented in the previous section are solved.

If this is the case, a similar method can be used to evaluate the expected rate and spectrum due to the soft protons for any new X-ray mission with focusing telescope as Athena, and the validation of the XMM-Newton matrix would automatically gives credit to the predicted rates.

Acknowledgements The results described in this paper have been reported during the AHEAD background workshop, organised with the support of the EU Horizon 2020 Programme (grant agreement n. 654215)

References

S. Agostinelli, J. Allison, K. Amako, J. Apostolakis, H. Araujo, P. Arce, M. Asai, D. Axen, S. Banerjee, G. Barrand, F. Behner, L. Bellagamba, J. Boudreau, L. Broglia, A. Brunengo, H. Burkhardt, S. Chauvie, J. Chuma, R. Chytracek, G. Cooperman, G. Cosmo, P. Degtyarenko, A. Dell'Acqua, G. Depaola, D. Dietrich, R. Enami, A. Feliciello, C. Ferguson, H. Fesefeldt, G. Folger, F. Foppiano, A. Forti, S. Garelli, S. Giani, R. Giannitrapani, D. Gibin, J.J. Gómez Cadenas, I. González, G. Gracia Abril, G. Greeniaus, W. Greiner, V. Grichine, A. Grossheim, S. Guatelli, P. Gumplinger, R. Hamatsu, K. Hashimoto, H. Hasui, A. Heikkinen, A. Howard, V. Ivanchenko, A. Johnson, F.W. Jones, J. Kallenbach, N. Kanaya, M. Kawabata, Y. Kawabata, M. Kawaguti, S. Kelner, P. Kent, A. Kimura, T. Kodama, R. Kokoulin, M. Kossov, H. Kurashige, E. Lamanna, T. Lampén, V. Lara, V. Lefebure, F. Lei, M. Liendl, W. Lockman, F. Longo, S. Magni, M. Maire, E. Medernach, K. Minamimoto, P. Mora de Freitas, Y. Morita, K. Murakami, M. Nagamatu, R. Nartallo, P. Nieminen, T. Nishimura, K. Ohtsubo, M. Okamura, S. O'Neale, Y. Oohata, K. Paech, J. Perl, A. Pfeiffer, M.G. Pia, F. Ranjard, A. Rybin, S. Sadilov, E. Di Salvo, G. Santin, T. Sasaki, N. Savvas, Y. Sawada, S. Scherer, S. Sei, V. Sirotenko, D. Smith, N. Starkov, H. Stoecker, J. Sulkimo, M. Takahata, S. Tanaka, E. Tcherniaev, E. Safai Tehrani, M. Tropeano, P. Truscott, H. Uno, L. Urban, P. Urban, M. Verderi, A. Walkden, W. Wander, H. Weber, J.P. Wellisch, T. Wenaus, D.C. Williams, D. Wright, T. Yamada, H. Yoshida, D. Zschiesche, G EANT4 Collaboration, GEANT4-a simulation toolkit. Nuclear Instruments and Methods in Physics Research A **506**, 250–303 (2003). doi:10.1016/S0168-9002(03)01368-8

J. Allison, K. Amako, J. Apostolakis, H. Araujo, P. Arce Dubois, M. Asai, G. Barrand, R. Capra, S. Chauvie, R. Chytracek, G.A.P. Cirrone, G. Cooperman, G. Cosmo, G. Cuttone, G.G. Daquino, M. Donszelmann, M. Dressel, G. Folger, F. Foppiano, J. Generowicz, V. Grichine, S. Guatelli, P. Gumplinger, A. Heikkinen, I. Hrivnacova, A. Howard, S. Incerti, V. Ivanchenko, T. Johnson, F. Jones, T. Koi, R. Kokoulin, M. Kossov, H. Kurashige, V. Lara, S. Larsson, F. Lei, O. Link, F. Longo, M. Maire, A. Mantero, B. Mascialino, I. McLaren, P. Mendez Lorenzo, K. Minamimoto, K. Murakami, P. Nieminen, L. Pandola, S. Parlati, L. Peralta, J. Perl, A. Pfeiffer, M.G. Pia, A. Ribon, P. Rodrigues, G. Russo, S. Sadilov, G. Santin, T. Sasaki, D. Smith, N. Starkov, S. Tanaka, E. Tcherniaev, B. Tome, A. Trindade, P. Truscott, L. Urban, M. Verderi, A. Walkden, J.P. Wellisch, D.C. Williams, D. Wright, H. Yoshida, Geant4 developments and applications. IEEE Transactions on Nuclear Science **53**, 270–278 (2006). doi:10.1109/TNS.2006.869826

J. Allison, K. Amako, J. Apostolakis, P. Arce, M. Asai, T. Aso, E. Bagli, A. Bagulya, S. Banerjee, G. Barrand, B.R. Beck, A.G. Bogdanov, D. Brandt, J.M.C. Brown, H. Burkhardt, P. Canal, D. Cano-Ott, S. Chauvie, K. Cho, G.A.P. Cirrone, G. Cooperman, M.A. Cortés-Giraldo, G. Cosmo, G. Cuttone, G. Depaola, L. Desorgher, X. Dong, A. Dotti, V.D. Elvira, G. Folger, Z. Francis, A. Galoyan, L. Garnier, M. Gayer, K.L. Genser, V.M. Grichine, S. Guatelli, P. Guèye, P. Gumplinger, A.S. Howard, I. Hřivnáčová, S. Hwang, S. Incerti, A. Ivanchenko, V.N. Ivanchenko, F.W. Jones, S.Y. Jun, P. Kaitaniemi, N. Karakatsanis, M. Karamitrosi, M. Kelsey, A. Kimura, T. Koi, H. Kurashige, A. Lechner, S.B. Lee, F. Longo, M. Maire, D. Mancusi, A. Mantero, E. Mendoza, B. Morgan, K. Murakami, T. Nikitina, L. Pandola, P. Paprocki, J. Perl, I. Petrović, M.G. Pia, W. Pokorski, J.M. Quesada, M. Raine, M.A. Reis, A. Ribon, A. Ristić Fira, F. Romano, G. Russo, G. Santin, T. Sasaki, D. Sawkey, J.I. Shin, I.I. Strakovsky, A. Taborda, S. Tanaka, B. Tomé, T. Toshito, H.N. Tran, P.R. Truscott, L. Urban, V. Uzhinsky, J.M. Verbeke, M. Verderi, B.L. Wendt, H. Wenzel, D.H. Wright, D.M. Wright, T. Yamashita, J. Yarba, H. Yoshida, Recent developments in GEANT4. Nuclear Instruments and Methods in Physics Research A **835**, 186–225 (2016). doi:10.1016/j.nima.2016.06.125

H. Bethe, Zur Theorie des Durchgangs schneller Korpuskularstrahlen durch Materie. Annalen der Physik **397**, 325–400 (1930). doi:10.1002/andp.19303970303

G. Conti, E. Mattaini, E. Santambrogio, B. Sacco, G. Cusumano, O. Citterio, H.W. Braeuninger, W. Burkert, X-ray characteristics of the Italian X-Ray Astronomy Satellite (SAX) flight mirror units, in *Advances in Multilayer and Grazing Incidence X-Ray/EUV/FUV Optics*, ed. by R.B. Hoover, A.B. Walker Proc. SPIE, vol. 2279, 1994, pp. 101–109. doi:10.1117/12.193179

G. Cusumano, S. Campana, P. Romano, V. Mangano, A. Moretti, A.F. Abbey, L. Angelini, A.P. Beardmore, D.N. Burrows, M. Capalbi, G. Chincarini, O. Citterio, P. Giommi, M.R. Goad, O. Godet, G.D. Hartner, J.E. Hill, J.A. Kennea, V. La Parola, T. Mineo, D. Morris, J.A. Nousek, J.P. Osborne, K. Page, C. Pagani, M. Perri, G. Tagliaferri, F. Tamburelli, A. Wells, In-flight calibration of the Swift XRT effective area, in *Gamma-Ray Bursts in the Swift Era*, ed. by S.S. Holt, N. Gehrels, J.A. Nousek American Institute of Physics Conference Series, vol. 836, 2006, pp. 664–667. doi:10.1063/1.2207972

M.A. Dayeh, M.I. Desai, J.R. Dwyer, H.K. Rassoul, G.M. Mason, J.E. Mazur, Composition and Spectral Properties of the 1 AU Quiet-Time Suprathermal Ion Population During Solar Cycle 23. Astrophys. J. **693**, 1588–1600 (2009). doi:10.1088/0004-637X/693/2/1588

S. Diebold, C. Tenzer, E. Perinati, A. Santangelo, M. Freyberg, P. Friedrich, J. Jochum, Soft proton scattering efficiency measurements on x-ray mirror shells. Experimental Astronomy **39**, 343–365 (2015). doi:10.1007/s10686-015-9451-4

B. Dorman, K.A. Arnaud, Redesign and Reimplementation of XSPEC, in *Astronomical Data Analysis Software and Systems X*, ed. by F.R. Harnden Jr., F.A. Primini, H.E. Payne Astronomical Society of the Pacific Conference Series, vol. 238, 2001, p. 415

O.B. Firsov, Reflection of Fast Ions from a Dense Medium at Glancing Angles. Soviet Physics Doklady **11**, 732 (1967)

F. Jansen, D. Lumb, B. Altieri, J. Clavel, M. Ehle, C. Erd, C. Gabriel, M. Guainazzi, P. Gondoin, R. Much, R. Munoz, M. Santos, N. Schartel, D. Texier, G. Vacanti, XMM-Newton observatory. I. The spacecraft and operations. Astron. Astrophys. **365**, 1–6 (2001). doi:10.1051/0004-6361:20000036

A. Leccardi, S. Molendi, Radial temperature profiles for a large sample of galaxy clusters observed with XMM-Newton. Astron. Astrophys. **486**, 359–373 (2008). doi:10.1051/0004-6361:200809538

D.H. Lo, J.R. Srour, Modeling of proton-induced CCD degradation in the Chandra X-ray observatory. IEEE Transactions on Nuclear Science **50**, 2018–2023 (2003). doi:10.1109/TNS.2003.820735

R.A. Mewaldt, C.M.S. Cohen, G.M. Mason, D.K. Haggerty, M.I. Desai, Long-Term Fluences of Solar Energetic Particles from H to Fe. Space Sci. Rev. **130**, 323–328 (2007). doi:10.1007/s11214-007-9200-8

V.S. Remizovich, M.I. Ryazanov, I.S. Tilinin, Energy and angular distributions of particles reflected in glancing incidence of a beam of ions on the surface of a material. Soviet Journal of Experimental and Theoretical Physics **52**, 225 (1980)

M.C. Weisskopf, B. Brinkman, C. Canizares, G. Garmire, S. Murray, L.P. Van Speybroeck, An overview of the performance and scientific results from the chandra x-ray observatory. PASP **114**, 1–24 (2002). doi:10.1086/338108